Journal of Metals, Materials and Minerals, Vol. 31, No. 3, pp. 100-105, 2021

Effects of ball milling duration and sintering temperature on mechanical alloying Fe_3Si

Varistha CHOBPATTANA[1], Chakansin PHOOMKONG[1], Peerawat NUTNUAL[1], Kritsada THAENGTHONG[2], and Wanchai PIJITROJANA[2,*]

[1] *Department of Materials and Metallurgical Engineering, Faculty of Engineering, Rajamangala University of Technology Thanyaburi, 39 Moo 1, Rangsit-Nakhon Nayok Road, Khlong Hok, Khlong Luang District, Pathum Thani 12110, Thailand*

[2] *Department of Electrical and Computer Engineering, Faculty of Engineering, Thammasat University, 99 Moo 18, Khlong Nueng, Khlong Luang District, Pathum Thani 12120, Thailand*

***Corresponding author e-mail:** pwanchai@engr.tu.ac.th

Received date:
14 March 2021
Revised date
16 June 2021
Accepted date:
21 June 2021

Keywords:
Fe_3Si alloy;
Ferromagnetic materials;
Powder metallurgy

Abstract

Fe_3Si is under interest as a ferromagnetic electrode of magnetic tunneling junctions (MTJs). Its crystalline structure is important for achieving high device efficiency. This work focuses on mechanical alloying of 3:1 ratio of 99% pure Fe and Si powder mixtures by ball milling and sintering. The mixtures were ball-milled for various durations up to 20 h. Then, they were sintered from 400°C to 800°C for 4 h in Ar. SEM images and particle size analysis show significant reduction in average particle size of the mixtures after ball milling for 20 h. The longer duration of ball milling process promotes powder distribution. It results in agglomerated and smooth samples after sintering. XRD analysis indicates that Fe_3Si phase appeared after 5 h of mechanical ball milling without sintering. More peaks of Fe_3Si phase present at sintering temperatures higher than 600°C, while Fe_2Si phase diminishes. However, the amount of Fe_2O_3 phase increases when sintering at these high temperatures, which strongly affects the magnetic properties of the samples. Magnetic hysteresis loops measured by vibrating-sample magnetometer (VSM) show lower magnetic moments of these samples. Saturation magnetization of the sample decreases more than 95% when sintered at 800°C, agreeing with high content of Fe_2O_3.

1. Introduction

The magnetoelectronic devices based on spin-polarized transport in semiconductors are obtained much attention at present. The spin-polarized carrier injection from a ferromagnetic (FM) source into a semiconductor offers new perspectives to semiconductor device technology. The spin-polarized based devices, such as light-emitting diodes (LEDs) using FM metals or FM semiconductors like (Ga, Mn)As as a spin injection source, are reported [1-4]. From Lin *et al*. [5], the authors propose, as for the spin-polarized Si-based LEDs, ferromagnetic Fe_3Si to be a good candidate for a spin-polarized carrier source on semiconducting Si. The other examples are the devices based on the Magnetic Tunneling Junction (MTJs) using FM metals for the electrodes sandwiching the barrier. The ferromagnetic Fe_3Si was proposed as an alternative for ferromagnetic electrodes as reported by W. Rotjanapittayakul *et al*., [6]. Fe_3Si is known to be ferromagnetic up to 840 K [7] with a cubic DO_3 structure regarded as a Heusler alloy [8]. In additions, Fe_3Si also has high spin polarization expected at the Fermi level [9]. Thus, Fe_3Si is an attractive material for electrical spin injection [10]. This Heusler alloy possesses relatively high saturation magnetization and low Gilbert damping parameter [6]. Development of Fe_3Si can be used in spintronics and nanoelectronics. Recent theoretical study of Fe_3Si-based magnetic tunnel junction showed promisingly results [11-19]. All of these studies focus on epitaxially growth thin films. Some other methods are chosen to obtain Fe-Si alloys including thermal evaporation, diffusion-driven annealing, magnetron sputtering, or mechanical alloying [20-23]. Mechanical alloying is an accessible approach to achieve polycrystalline structure from amorphous or monocrystalline powder mixture. The process can develop different properties for the poly-crystalline materials including advance electrical, thermal and magnetic properties. In this paper, we demonstrate the mechanical alloying method to synthesize Fe_3Si Heusler Alloy. Subsequent sintering step can further provide desirable crystalline phases driving to the potential properties. Phase diagram of Fe-Si suggests that α-Fe_3Si phase can be formed between 10 at% to 25 at% Si at temperature range 500°C to 900°C, which is thermodynamically preferred over off-stoichiometry alloys. Previous work has been done on low Si content [23]. According to this limitation, mixture of slightly higher Si content is examined in this study for the mechanically alloy process in order to achieve higher electrical resistivity [24]. It is suggested that long duration of mechanically alloying could produce Fe_3Si phase even at low sintering temperature.

2. Experimental setup

14 wt% mixture of high purity (99%) Fe and Si powders (Labchem, <44 μm) were ball-milled at 1200 rpm for 0, 1, 3, 5, 10, and 20 h. Then, the mixtures were sintered in a tube furnace (Carbolite-

Gero, Germany) at 400, 600, and 800°C in Ar atmosphere for 5 h. Morphologies of the samples were investigated by optical microscope and scanning electron microscope (SEM, JEM-6510, JEOL). Particle size analysis was performed via ImageJ. Crystallographic structures were characterized by x-ray diffraction (XRD, Cu-Ka, X'Pert PRO MPD model pw 3040/60, PANalytical) using CuKα (wavelength = 0.154 nm). Vibrating-sample magnetometry was performed at room temperature to analyze the magnetic properties of the mixtures. Maximum magnetic field was 10 T.

3. Results and discussions

3.1 Effect of ball-milling time

Effect of ball-milling time on the particle size is studied by comparing the microstructure of the particles. As shown in SEM micrographs in Figure 1, the sizes of the particles decrease as the milling durations increase. The particles of the 5-h ball-milled mixture (Figure 1(a)) are connected in large groups. On the other hand, for the 20-h ball-milled mixture, the particles are dispersed as individual parts (Figure 1(b)). The average particle sizes of the 5-h and 20-h ball-milled samples are 25.46 μm and 8.2 μm, respectively. Particle size distributions of the ball-milled samples are illustrated in Figure 2. Mean particle size is reported between 11 μm to 20 μm. The comminution suggests that the mechanical ball milling reduces the particle size of the powder. It can be observed that the samples are fragile, and the mixtures remain powder after ball milling for 20 h. It is common that Fe-Si alloys with more than 4.5% silicon are brittle. However, after sintering at 600°C and 800°C, the powder at both conditions are fused firmly into one rigid piece, without external compression step. It is also implied that the smaller particle size allowing denser packed compound. This behavior accommodates the aggregation of the particles during sintering. At very small particle size, particles behave more ductile [25]. It was suggested that small particles tend to form aggregates to reduce their surface energy [26]. As a result, the high temperature sintering confers higher strength and integrity to the sample structure.

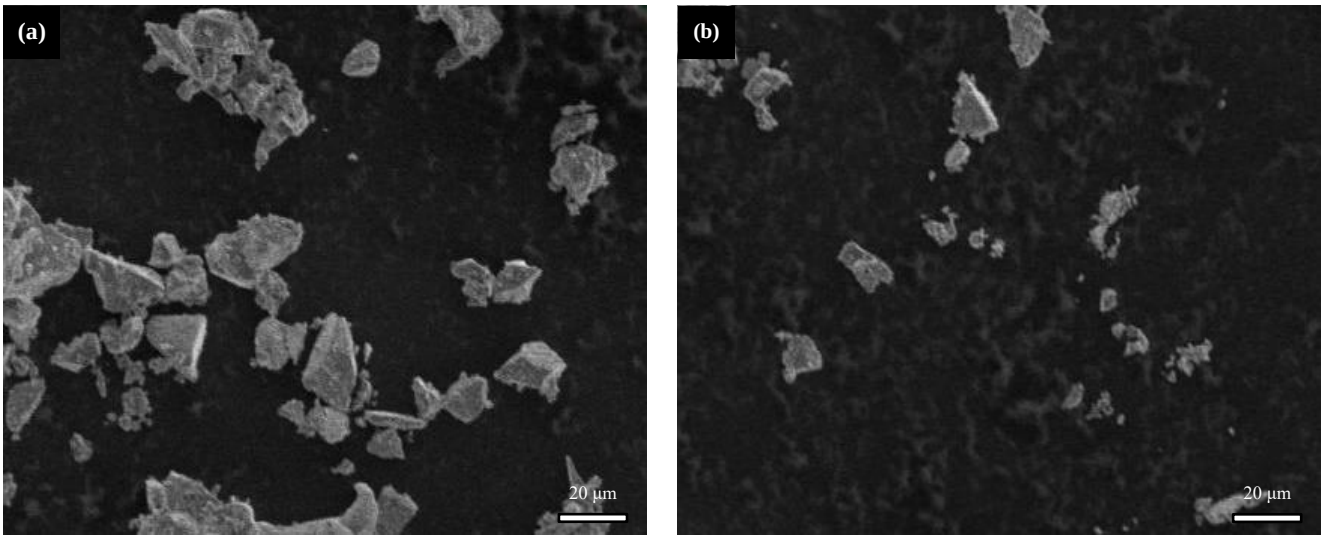

Figure 1. Fe-Si powder alloys after (a) 5 h, and (b) 20 h mechanical annealing.

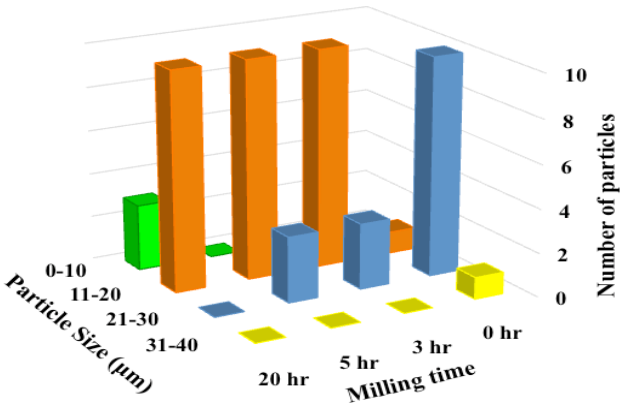

Figure 2. Particle size distribution of the ball-milled samples with various ball milling time.

In addition, surface morphology indicates that the durations of ball milling influence Fe and Si particles distribution. The two species are more evenly distributed as extending the milling time. Figure 3 presents surface of Fe-Si mixture after annealing at 800°C in Ar with different mechanical ball-milling durations. It is noted that each samples consolidate as a solid piece after high temperature sintering. Figure 3(a) displays surface of a sample with no mechanical ball milling. The particle sizes are large and separated comparing to the 3-h ball-milled samples shown in Figure 3(b), which presents finer and evenly distributed grains. The surface of the 5-h ball-milled sample in Figure 3(c) appears fine and smooth. Lastly, the 20-h ball-milled sample in Figure 3(d) features glossy and shiny. Some parts of these samples demonstrate that particles are fused into large grains. It was observed that the harder component is embedded in the softer component during milling [25]. Thus, the harder Si particles would be surrounded by Fe particles. The observation of the surface agrees with the microstructure of the 20-h ball-milled sample shown in Figure 4. The particles are connected into large granules. The result suggests phase change starts on the samples with the longer milling time, which can be examined with crystallinity analysis.

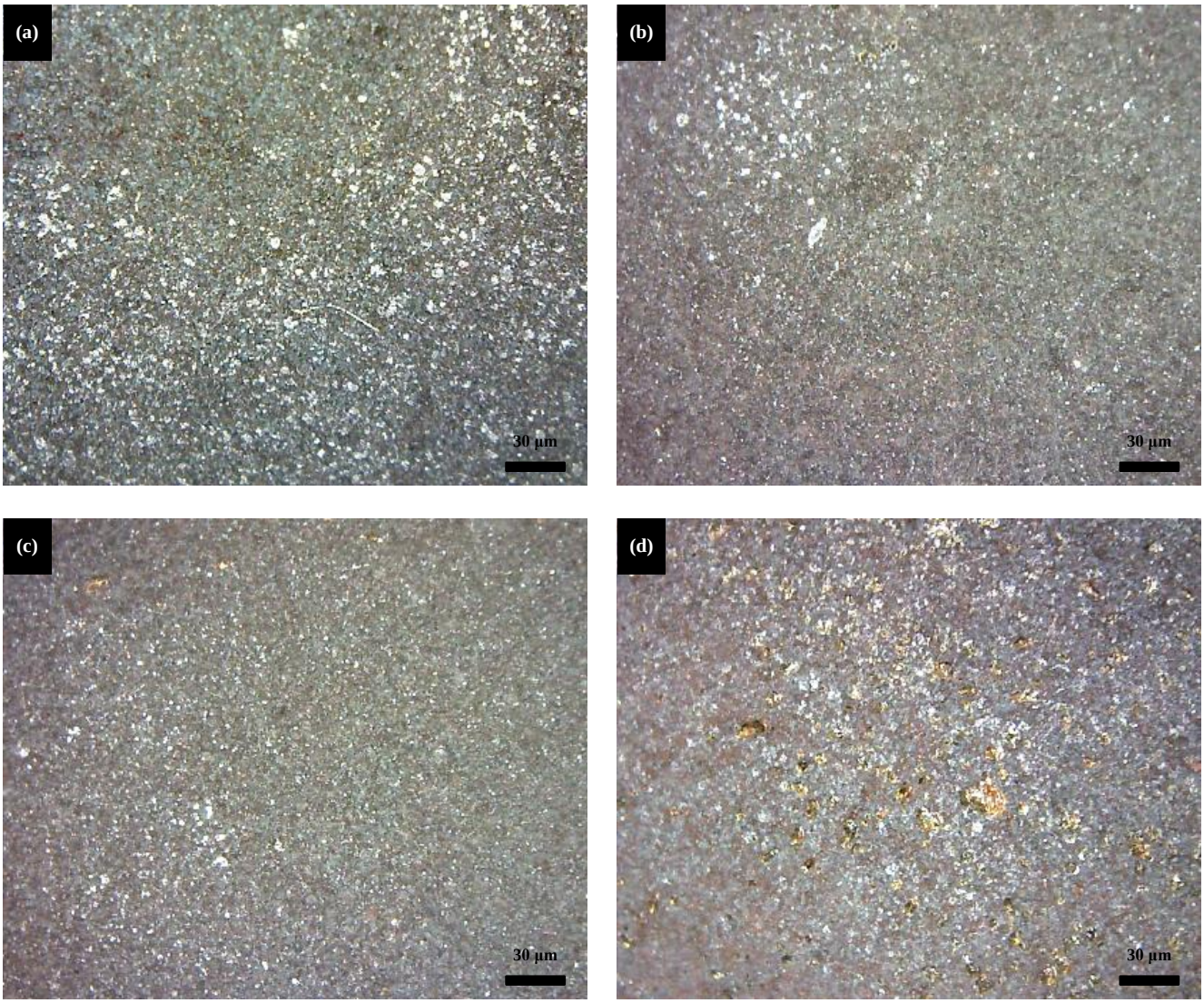

Figure 3. Surface morphology of Fe-Si mixture after sintering at 800°C in Ar with (a) no mechanical milling, (b) 3 h, (c) 5 h, and (d) 20 h of mechanical milling.milling.

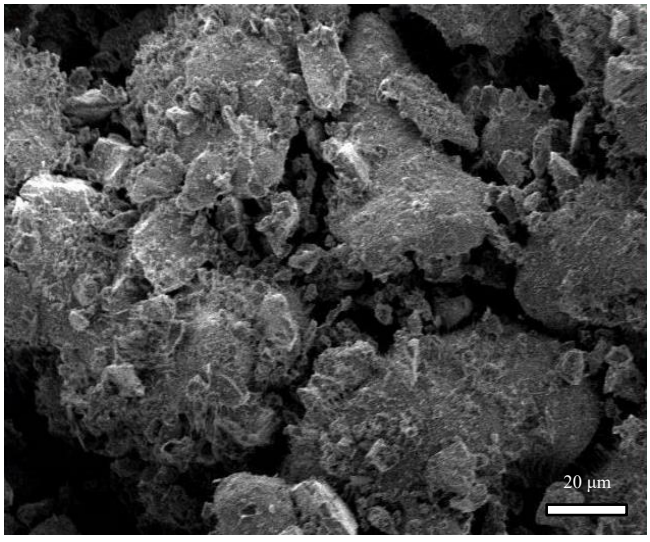

Figure 4. Microstructure of Fe-Si mixture after sintering at 800°C in Ar with 20 h of mechanical milling.

3.2 Effect of sintering temperature

For phase analysis, XRD spectra of 3-h of mechanically ball-milled samples with various sintering temperatures are shown in Figure 5. The 3-h and 5-h ball-milled samples exhibit similar patterns. Peaks of Fe-Si alloys were identified relating to their diffracting angles. FeSi and Fe_2Si phases present even with no sintering. After sintering at 400°C, Fe_2Si peak emerges at 35.6°. Main difference in both sets of samples arises at transition temperature between 400°C and 600°C. The peak intensity at 35.6° appears much stronger, which correspond to larger grain size [27]. At 600 and 800°C, Fe_3Si peaks occurs at 54.13° and 76.42°, while other Si and Fe_2Si peaks disappear. In addition, the amount of Fe_2O_3 substantially rises at the high sintering temperature. There is no Fe_2O_3 presented at 400°C.

Table 1 shows the amount of each phase in the samples. The analysis from the 3-h ball-milled samples suggested that Fe_2Si is formed from the mechanical ball milling. Moreover, the presence of Fe_2Si, and Fe_3Si amount suggests that the alloys are already developed after 5-h of mechanical ball milling. Long milling time

incites Fe-Si formation for as-milled powder [23]. Moreover, both cases show low amount of Fe compared to Si, indicating that more amounts of Fe_2Si and Fe_3Si are formed comparing to FeSi. From 25°C to 400°C transition, the amount of FeSi phase increases in both series, while the Fe:Si ratio decreases.

During the transitions from 400°C to 600°C, while the other phases (Fe, Fe_2Si, and Fe_3Si) decline significantly, the amount of Si phase remains relatively constant for the 3-h ball-milled sample sintered at 600°C. The behavior implied that only Fe is oxidized at this condition. However, when the duration of the ball-milling time is lengthened, the amount of Si decreases. More than 50% of the mixture is assigned to Fe_2O_3 for the 5-h ball-milled sample sintered at 600°C. The reduction in Si amount indicates that Si is also oxidized. This behavior also displays for the 3-h ball-milled samples at higher temperature. For 600°C to 800°C transition, the amount of Si of this set of samples drops from 51.2% to 41.1%, while the amount of Fe_2O_3 surges from 39.3% to 48.2%. However, Fe_2O_3 changes only from 53.3% to 59.8% in the 5-h ball-milled sample. The behavior suggests that longer mechanical ball milling duration influences oxidation at lower sintering temperature for Fe-Si alloying.

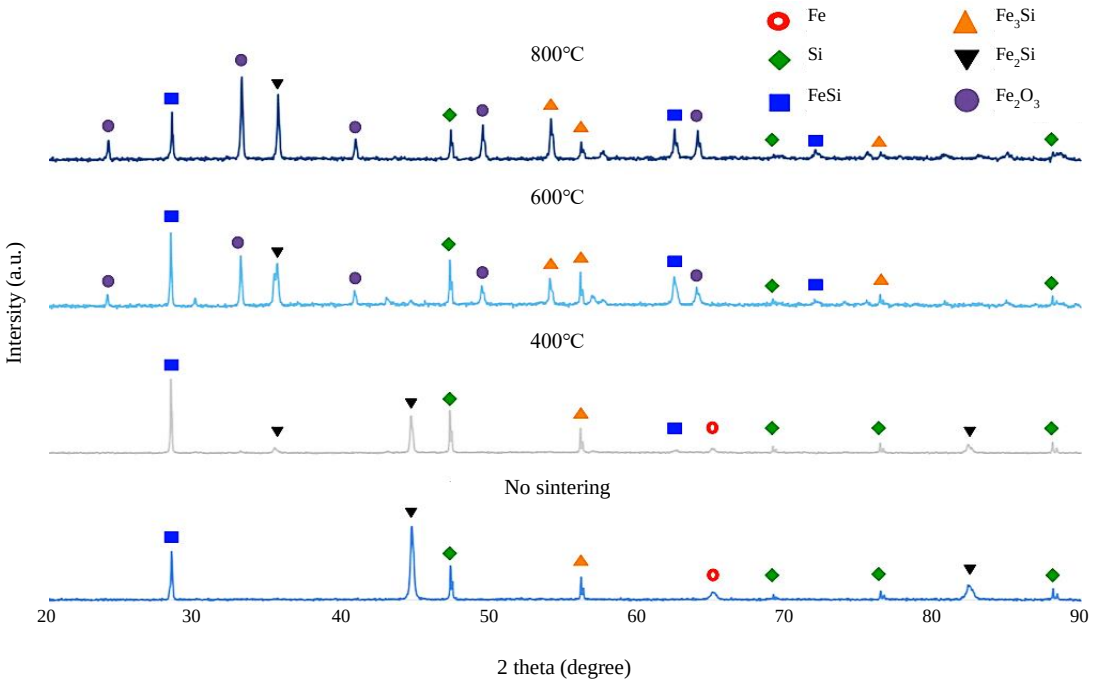

Figure 5. XRD spectra of 3-h mechanically ball-milled samples with different sintering temperatures.

Table 1. Different phases presented in the Fe-Si mixtures.

Sample	Amount (%)					
	Fe	**Si**	**FeSi**	**Fe_3Si**	**Fe_2Si**	**Fe_2O_3**
3 hr 25°C	42.2	43.1	0.1	1.5	13.0	-
5 hr 25°C	14.9	49.1	4.3	17.0	14.7	-
3 hr 400°C	23.0	49.7	15.2	9.0	3.1	-
5 hr 400°C	13.3	58.1	10.3	11.4	15.6	-
3 hr 600°C	1.5	51.2	1.5	6.1	0.4	39.3
5 hr 600°C	1.2	31.4	5.0	6.2	0.9	53.3
3 hr 800°C	0.9	41.1	0.1	8.0	1.8	48.2
5 hr 800°C	0.7	30	1.3	6.2	1.2	59.9

Magnetic hysteresis loops are measured by vibrating-sample magnetometer (VSM). The results exhibit the existence of a ferromagnetic state of these samples. Figure 6 presents the comparison of hysteresis curves of the 3-h (Figure 6(a)) and the 5-h ball-milled samples (Figure 6(b)) with various sintering temperatures. The analysis reveals that saturation magnetization (M_s) of the samples decreases as the sintering temperature increases, regardless of the ball-milling time. This investigation agrees with the XRD analysis. The longer milling duration gives rise to the Fe-Si formation, which has been shown to decrease M_s [23]. The drop in the M_s corresponds to the growth of Fe_2O_3 phase of the samples sintered at 600 and 800°C. By using this method, the M_s remains relatively similar for the samples sintered up to 400°C. The mean of the M_s of the samples sintered up to 400°C is about 169 emu·g^{-1} which is close to that of bulk Fe_3Si [28]. The M_s of the sample plunges more than 95% when sintered at 800°C, agreeing with high content of Fe_2O_3. In addition, rising ball-milling time slightly decreases the M_s of the samples, as the magnitude is shown in the inset of Figure 6.

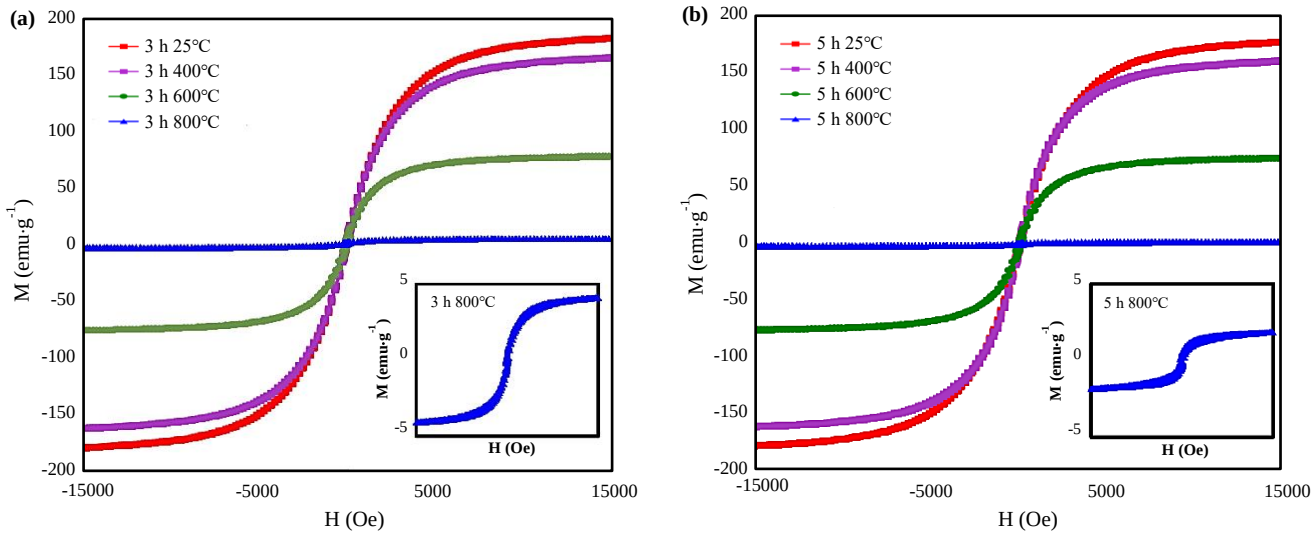

Figure 6. Hysteresis curve of Fe-Si mixture ball-milled for (a) 3 h and (b) 5 h and sintered at 25, 400, 600, and 800°C in Ar atmosphere.

Table 2. Magnetic properties of samples.

Sample	M_s (emu·g^{-1})	B_r (emu·g^{-1})	H_c (Oe)
3 h 25°C	179.1	1.06	14.25
5 h 25°C	176.5	1.10	14.91
3 h 400°C	162.1	1.13	15.92
5 h 400°C	159.8	0.38	5.47
3 h 600°C	76.13	3.67	70.79
5 h 600°C	75.09	3.62	68.04
3 h 800°C	4.11	0.43	140.9
5 h 800°C	1.85	0.44	264.4

The M_s, remanance flux (B_r), and magnetic coercivity forces (H_c) of the 3-h and 5-h ball-milled samples sintered at 25, 400, 600, and 800°C are shown in Table 2. All of the 3-h ball-milled samples display higher M_s than that of the 5-h ball-milled samples, which indicates slightly stronger polarization. This result also correlates to the effect of longer milling duration on the oxidation of Si. The magnitization reduces significantly at 800°C as Fe and Si oxidized. The H_c of the samples sintered at 25°C and 400°C are small since the samples are in the form of bulk Fe_3Si. Noticeably, it escalates for the higher sintering temperature. This behavior implies that the samples are formed similar to most thin magnetic films, which the H_c of Fe_3Si films intensifies with decreasing thickness [29]. According to Liou *et al*. [29], the H_c of Fe_3Si films reaches a maximum for the film 10 ML (monolayer) thick, as high as 500 Oe. It was suggested that the increasing in H_c with milling time was due to the reduction in the particle size and the introduction of dislocations [30].

4. Conclusions

The facile mechanical annealing has proven to provide the Fe_3Si alloy. The influence of the ball-milling time and sintering temperature were investigated on crystallinity and magnetic properties of Fe-Si alloys. Microstructural study shows that the process yields evenly distributed particles, leading to formation of the Fe-Si alloys. XRD results indicate that Fe_3Si phase can be achieved from mechanically alloying the Fe-Si powder mixture for 5 h at room temperature. Mechanically ball milling influences oxidation of the Fe-Si mixtures even at low sintering temperature. As the oxidation dominates at high temperature, the alloy mixture results in high amount for Fe_2O_3. Correspondingly, the saturation magnetization falls at 800°C. In addition, increasing ball milling time slightly lowers the maximum magnetization of the samples. For further study, it is suggested that closed annealing system is recommended to avoid oxidation.

Acknowledgements

The authors gratefully acknowledge the financial support provided by Thammasat University Research Fund under the TU innovative Scholar, Contact No. IS 8/2561. A portion of this work was performed in Rajamangala University of Technology, Thanyaburi, RMUTT's central laboratory.

References

[1] R. Fiederling, M. Keim, G. Reuscher, W. Ossau, G. Schmidt, A. Waag, and L.W. Molenkamp, "Injection and detection of a spin-polarized current in a light-emitting diode," *Nature*, vol. 402, pp. 787-790, 1999.

[2] Y. Ohno, D.K. Young, B. Beschoten, F. Matsukura, H. Ohno, and D.D. Awschalom, "Electrical spin injection in a ferro-

magnetic semiconductor heterostructure," *Nature*, vol. 402, pp. 790-792, 1999.

[3] B.T. Jonker, Y.D. Park, B.R. Bennett, H.D. Cheong, G. Kioseoglou, and A. Petrou, "Robust electrical spin injection into a semiconductor heterostructure," *Physical Review B*, vol. 62, pp. 8180-8183, 2000.

[4] T. Manago, and H. Akinaga, "Spin-polarized light-emitting diode using metal/insulator/semiconductor structures," Applied Physics Letters, vol. 81, pp. 694-696, 2002.

[5] F. Lin, D. Jiang, X. Ma, and W. Shi, "Structural order and magnetic properties of Fe_3Si/Si(100) heterostructures grown by pulsed-laser deposition," *Thin Solid Films*, vol. 515, pp. 5353-5356, 2007.

[6] W. Rotjanapittayakul, W. Pijitrojana, T. Archer, S. Sanvito, and J. Prasongkit, "Spin injection and magnetoresistance in MoS_2-based tunnel junctions using Fe_3Si Heusler alloy electrodes," *Scientific Reports*, vol. 8, pp. 4779, 2018.

[7] S.H. Liou, S.S. Malhotra, J.X. Shen, M. Hong, J. Kwo, H.S. Chen, and J.P. Mannaerts, "Magnetic properties of epitaxial single crystal ultrathin Fe_3Si films on GaAs (001)," *Applied Physics Letters*, vol. 73, no. 10, pp. 6766-6768, 2003.

[8] W.A. Hines, A.H. Menotti, J.I. Budnick, T.J. Burch, T. Litrenta, V. Niculescu, and K. Raj, "Magnetization studies of binary and ternary alloys based on Fe_3Si," *Physical Review B*, vol. 13, no. 9, pp. 4060-4068, 1976.

[9] R.A. de Groot, and F.M. Mueller, "New Class of Materials: Half-Metallic Ferromagnets," *Physical Review Letters*, vol. 50, no. 25, pp. 2024-2027, 1983.

[10] A. Kawaharazuka, M. Ramsteiner, J. Herfort, H.-P. Schonherr, H. Kostial, and K.H. Ploog, "Spin injection from Fe_3Si into GaAs," *Applied Physics Letters*, vol. 85, no. 16, pp. 3492-3494, 2004.

[11] Y. Fujita, S. Yamada, G. Takemoto, S. Oki, Y. Maeda, M. Miyao, and K. Hamaya, "Room-temperature tunneling magneto-resistance in magnetic tunnel junctions with a $D0_3$ – Fe_3Si electrode," *Japanese Journal of Applied Physics*, vol. 52, number 4S, 2013.

[12] K. Kobayashi, T. Suemasu, N. Kuwano, D. Hara, and H. Akinaga, "Epitaxial growth of $Fe_3Si/CaF_2/Fe_3Si$ magnetic tunnel junction structures on CaF_2/Si (111) by molecular beam epitaxy," *Thin Solid Films*, vol. 515, pp. 8254-8258, 2007.

[13] K. Harada, K. Makabe, H. Akinaga, and T. Suemasu, "Magneto-resistance characteristics of $Fe_3Si/CaF_2/Fe_3Si$ heterostructures grown on Si (111) by molecular beam epitaxy," *Physics Procedia.* vol. 11, pp.15-18, 2011.

[14] K. Harada, K. Makabe, H. Akinaga, and T. Suemasu, "Room temperature magnetoresistance in $Fe_3Si/CaF_2/Fe_3Si$ MTJ epitaxially grown on Si (111)," *Journal of Physics: Conference Series*, vol. 266, pp. 0120881-0120885, 2011.

[15] L.L. Tao, S.H. Liang, D.P. Liu, H.X. Wei, J. Wang, and X.F. Han, "Tunneling magnetoresistance in $Fe_3Si/MgO/Fe_3Si$ (001) magnetic tunnel junctions," *Applied Physics Letter*, vol.104, pp. 1724061-1724065, 2014.

[16] K. Ishibashi, K. Kudo, K. Nakashima, Y. Asai, K. Sakai, H. Deguchi, and T. Yoshitake, "Temperature-dependent magneto-resistance effects in $Fe_3Si/FeSi_2/Fe_3Si$ trilayered spin valve junctions," *Japan Society of Applied Physics Conference Proceedings*, vol. 5, pp. 011501, 2017.

[17] S. Gaucher, B. Jenichen, J. Kalt, U. Jahn, A Trampert, and J. Herfort, "Growth of $Fe_3Si/Ge/Fe_3Si$ trilayers on GaAs (001) using solid-phase epitaxy," *Applied Physics Letters*, vol. 110, pp. 102103, 2017.

[18] B. Jenichen, J. Herfort, U. Jahn, A. Trampert, and H. Riechert, "Epitaxial $Fe_3Si/Ge/Fe_3Si$ thin film multilayers grown on GaAs (001)," *Thin Solid Films*, vol. 556, pp. 120-124, 2014.

[19] H. Vinzelberg, J. Schumann, D. Elefant, E. Arushanov, and O.G. Schmidt, "Transport and magnetic properties of Fe_3Si epitaxial films," *Journal Applied Physics*, vol. 104, pp. 093707, 2008.

[20] J. Xie, Q. Xie, R. Ma, J. Huang, C. Zhang, and D. Liu, "Annealing temperature dependent structures and properties of ferromagnetic Fe_3Si films fabricated by resistive thermal evaporation," *Journal of Materials Science: Materials in Electronics*, vol.29, pp. 1369-1376, 2018.

[21] K. Seo, N. Bagkar, S. Kim, J. In, H. Yoon, Y. Jo, and B. Kim, "Diffusion-Driven Crystal Structure Transformation: Synthesis of Heusler Alloy Fe_3Si Nanowires," *Nano Letter*, vol. 10, pp. 3643-3647, 2010.

[22] T. Yoshitake, D. Nakagauchi, T. Ogawa, M. Itakura, N. Kuwano, Y. Tomokiyo, T. Kajiwara, and K. Nagayama, "Room-temperature epitaxial growth of ferromagnetic Fe_3Si films on Si(111) by facing target direct-current sputtering," *Applied Physics Letters*, vol. 86, pp. 262505, 2005.

[23] C.D. Stanciu, T.F. Marinca, I. Chicinas, and O. Isnard, "Characterisation of the Fe-10 wt% Si nanocrystalline powder obtained by mechanical alloying and annealing," *Journal of Magnetism and Magnetic Materials*, vol. 441, pp. 455-464, 2017.

[24] H. Gomi, K. Hirose, H. Akai, and Y. Fei, "Electrical resistivity of substitutionally disordered hcp Fe–Si and Fe–Ni alloys: chemically-induced resistivity saturation in the Earth's core", *Earth Planet. Sci. Letter*, vol. 451, pp. 51-61, 2016.

[25] C. Suryanarayana, "Mechanical alloying and milling" *Progress in Materials Science*, vol. 46, pp. 38, 2001.

[26] D. Walter, *Nanomaterials.* Deutsche Forschungsgemeinschaft (DFG), 2013.

[27] H. Yamada, H. Katsumata, D. Yuasa, S. Uekusa, M. Ishiyama, H. Souma, I. Azumaya, "Structural and electrical properties of β-$FeSi_2$ bulk materials for thermoelectric applications" *Physics Procedia*, vol 23, pp. 13-16, 2012.

[28] R. M. Bozorth, *Ferromagnetism*, New York: Van Nostrand, 1964.

[29] S. H. Liou, S. S. Malhotra, and J. X. Shen, "Magnetic properties of epitaxial single crystal ultrathin Fe_3Si films on GaAs (001)," *Journal of Applied Physics*, vol. 73, no. 10, pp. 6766-6768, 1993.

[30] M. P. C. Kalita, A. Perumal, and A. Srinivasan, "Structure and magnetic properties of nanocrystalline $Fe_{75}Si_{25}$ powders prepared by mechanical alloying," *Journal of Magnetism and Magnetic Materials*, vol. 320, no. 21, pp. 2780-2783, 2008.